# Scattering of Arbitrarily Polarized Plane Waves Obliquely Incident on Infinite Slots or Strips in a Planar-Stratified Medium

John L. Tsalamengas, *Member, IEEE*

***Abstract*—An exact analysis of three-dimensional scattering by a slot or by a strip right on an interface between two adjacent layers of a planar stratified isotropic medium is presented. The most general case of arbitrarily polarized obliquely incident plane waves is considered. The formulation is based on systems of singular integral-integrodifferential equations (SIE-SIDE). These systems are discretized with the help of two independent algorithms recently developed in [1]. Filling up the matrix elements involves rapidly convergent spectral integrals. The expression of the far-radiated field is derived and numerical results are presented for several cases.**

***Index Terms*— Electromagnetic scattering, nonhomogeneous media.**

## I. Introduction

THIS paper is concerned with electromagnetic diffraction by infinite strips or slots that reside on an interface between two adjacent layers (worst case) of a planar stratified linear isotropic medium. The most general case of arbitrarily polarized obliquely incident plane waves is considered.

Such problems are commonly formulated via a system of coupled integral equations of the first kind [(3), (6) below], which may be systematically derived using, for instance, the immittance approach [2].

The coupled character of the equations differs from the case of normal incidence wherein TE and TM (to strip/slot axis) waves decouple and can be treated separately by several analytical or numerical methods. For example, low/high-frequency techniques, dual-integral equations, moment methods, SIE, etc. (see [3]–[11] where further references are cited).

It is found in connection with this system that from the spectral integrals, which represent its kernels, one converges rather slowly (conditionally) while the other three diverge. To overcome this inconvenience, suitable singularity extraction procedures similar to those used in [8] and [9] are followed (see Sections III and IV). These procedures help recast the initial rather inconvenient kernels into sums of singular closed-form terms plus rapidly convergent spectral integrals. Discretization of these systems with the help of two independent, efficient algorithms recently developed in [1] enables filling up the matrix elements in terms of rapidly converging spectral integrals solely.

Manuscript received August 10, 1995; revised July 13, 1998.

The author is with the Department of Electrical and Computer Engineering, National Technical University of Athens, Athens, GR-157 73 Greece.

Publisher Item Identifier S 0018-926X(98)08882-6.

The following analysis is based on the $\exp(+j\omega t)$ time dependence, which is suppressed throughout.

## II. Basic Formulation

The geometry of the problem is shown in Fig. 1. The $i$th layer is characterized by the scalar constants $(\varepsilon_i, \mu_i, k_i = \omega\sqrt{\varepsilon_i\mu_i}), -n-1 \le i \le m+1$. The slot/strip is located at $y = 0$, $-w \le x \le w$, $-\infty < z < +\infty$.

The primary excitation is an arbitrarily polarized plane wave propagating in the direction of $\bar{k}^{\rm inc}(k_{m+1}, \Theta, \Phi)$ in the outmost region $(m+1)$. This wave is fully described in terms of its $z$ components

$$\left[E_z^{\rm inc}(\bar{r}), H_z^{\rm inc}(\bar{r})\right] = (E_0, H_0)\, e^{j\bar{k}^{\rm inc}\cdot\bar{r}} \tag{1}$$

where $E_0$ and $H_0$ denote field amplitudes and

$$\begin{aligned}\bar{k}^{\rm inc} &= k_{m+1}(\sin\Theta\sin\Phi\hat{x} + \cos\Theta\hat{y} + \sin\Theta\cos\Phi\hat{z}) \\ &= k_x\hat{x} + k_y\hat{y} + \beta\hat{z}.\end{aligned} \tag{2}$$

Let $[\bar{E}^{\rm exc}(\bar{r}), \bar{H}^{\rm exc}(\bar{r})] = [\bar{e}(y), \bar{h}(y)]\exp(jk_x x + j\beta z)$ denote the known [11] field excited by the incident wave when $w = 0$ (slot\strip absent). Then $[\bar{E}(x,y), \bar{H}(x,y)]\, e^{j\beta z} = [\bar{E}^{\rm tot}(\bar{r}), \bar{H}^{\rm tot}(\bar{r})] - [\bar{E}^{\rm exc}(\bar{r}), \bar{H}^{\rm exc}(\bar{r})]$, where $(\bar{E}^{\rm tot}, \bar{H}^{\rm tot})$ stands for the total field, defines the scattered field. In connection with the structure of Fig. 1(a), $\bar{M}(x) = \bar{E}(x,0)\times\hat{y} = \hat{z}E_x(x,0) - \hat{x}E_z(x,0) = \hat{x}M_x(x) + \hat{z}M_z(x)$ will be the equivalent surface magnetic current density across the slot. For the structure of Fig. 1(b), the induced current density on the strip will be denoted by $\bar{J}(x) = \hat{x}J_x(x) + \hat{z}J_z(x)$ (the $e^{j\beta z}$ factor has been suppressed for convenience).

For the configuration of Fig. 1(a) on the basis of the immittance-like approach outlined in Appendix A, the following system of two-coupled integral equations to $M_x$ and $M_z$

$$\begin{aligned}&\mathcal{K}^M(G_1, G_2; x) = h_x(0+)\, e^{jk_x x}, \\ &\mathcal{K}^M(G_2, G_3; x) = h_z(0+)\, e^{jk_x x} \quad (|x| \le w)\end{aligned} \tag{3}$$

is obtained. Here, $\mathcal{K}^M(G_i, G_j; x)$ stands for the shorthand notation

$$\begin{aligned}\mathcal{K}^M(G_i, G_j; x) = \frac{1}{2\pi}\int_{-w}^{w} dx' \int_{-\infty}^{\infty} e^{-ju(x-x')}[G_i(u)M_x(x') \\ + G_j(u)M_z(x')]\, du\end{aligned} \tag{4}$$

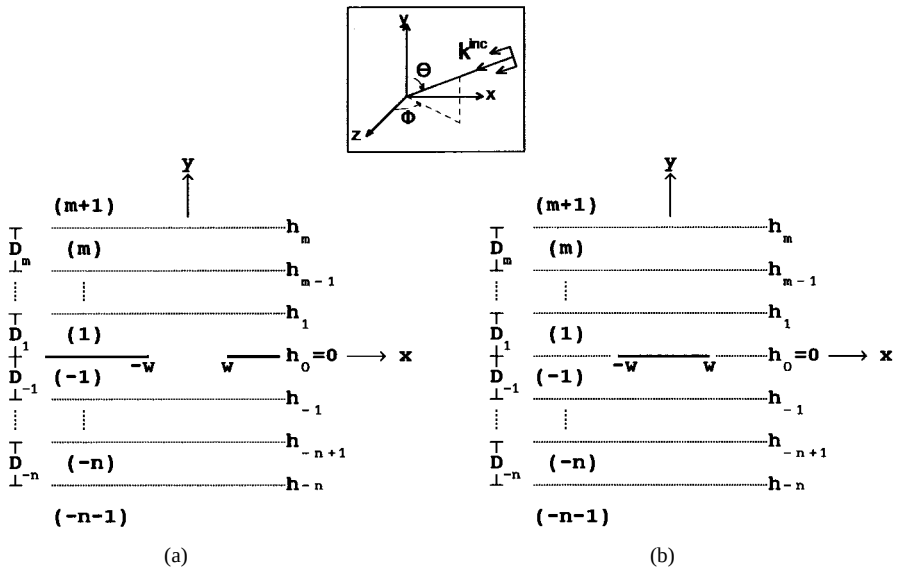


(a) (b)

Fig. 1. Geometry of a stratified medium loaded by (a) an infinitely thin slot and (b) an infinitely thin strip right on an interface between two layers.

$(i = 1,2; j = 2,3)$ where $G_j(u) = G_j(u;\Psi^e,\Psi^h)$ $(j = 1,2,3)$ are given by

$$G_1(u) = G_1(u;\Psi^e,\Psi^h) = \frac{-u^2\Psi^h + \beta^2\Psi^e}{\beta^2+u^2}$$
$$G_2(u) = u\beta\frac{\Psi^e+\Psi^h}{\beta^2+u^2}, \quad G_3(u) = \frac{u^2\Psi^e - \beta^2\Psi^h}{\beta^2+u^2} \tag{5}$$

with $\Psi^e(u)$ and $\Psi^h(u)$ defined in (42) in Appendix A.

For the structure of Fig. 1(b), the equations for $J_z$ and $J_x$ analogous to (3) are

$$\mathcal{K}^J(Z_1,Z_2;x) = e_x(0+)\,e^{jk_x x},$$
$$\mathcal{K}^J(Z_2,Z_3;x) = e_z(0+)\,e^{jk_x x} \tag{6}$$

$(|x| \le w)$ where $\mathcal{K}^J$ is given by (4) after setting $M \to J$ everywhere while

$$Z_j(u) = Z_j(u;\Psi^e,\Psi^h) = G_j(u;1/\Psi^e,1/\Psi^h). \tag{7}$$

Systems (3) and (6) will be treated separately in the following two sections.

## III. Reduction of (3) to a System of SIE-SIDE

Since $G_j(u)$ $(j = 1,2,3)$ vary as $|u|^{2-j}$ when $u \to \pm\infty$, (3) is rather impractical as it involves either divergent or (at best) conditionally convergent real-axis inverse Fourier integrals. To recast it into a convenient form we take advantage of the decompositions

$$\Psi^q(u) = \mathcal{Y}_1^q + \mathcal{Y}_0^q + Q^q(u) \quad (q = e,h)$$
$$G_j(u) = g_j(u) + G^{(j)}(u) \tag{8}$$

where $\mathcal{Y}_0^q$, $\mathcal{Y}_1^q$ are defined in (39) in Appendix A and

$$g_j(u) = G_j\big(u;\mathcal{Y}_1^e+\mathcal{Y}_0^e,\mathcal{Y}_1^h+\mathcal{Y}_0^h\big)$$
$$G^{(j)}(u) = G_j(u;Q^e,Q^h). \tag{9}$$

One may verify that $Q^e(u)$ and $Q^h(u)$ as well as $G^{(j)}(u)$ decay exponentially. On the other hand, although $g_j(u)$ continue to vary as $|u|^{2-j}$, the inverse Fourier integrals $\int_{-\infty}^{\infty} g_j(u)\,e^{-ju(x-x')}\,du$ can be evaluated in closed form. Leaving aside all intermediate derivations, (3) finally takes the following form of a system of singular integral-integrodifferential equations (SIE-SIDE) of the first kind

$$\mathcal{K}^M\big(G^{(1)},G^{(2)};x\big) - \sum_{s=0}^{1}\frac{1}{2\omega\mu_s}\left[j\beta\frac{d}{dx}\mathcal{M}_z^s(x) + \left(k_s^2+\frac{d^2}{dx^2}\right)\mathcal{M}_x^s(x)\right] = h_x(0+)\,e^{jk_x x} \tag{10a}$$

$$\mathcal{K}^M\big(G^{(2)},G^{(3)};x\big) - \sum_{s=0}^{1}\frac{1}{2\omega\mu_s}\left[j\beta\frac{d}{dx}\mathcal{M}_x^s(x) + \kappa_s^2\mathcal{M}_z^s(x)\right] = h_z(0+)\,e^{jk_x x} \tag{10b}$$

where

$$\kappa_s^2 = k_s^2 - \beta^2$$
$$\mathcal{M}_p^s(x) = \int_{-w}^{w} M_p(x')H_0^{(2)}(\kappa_s|x-x'|)\,dx' \quad (p \equiv x,z). \tag{11}$$

System (10) is of the type encountered in [1] and can be discretized using the algorithms explored there. In the following, two of these algorithms (termed methods A and B) will be independently applied.

### A. Disretization of (10) by Method A

We set $x = wt$, $x' = wt'$ $(-1 \le t,t' \le 1)$ and expand $M_z$ and $M_x$ in series of Chebyshev polynomials of the first and of the second kind

$$M_z[x(t)] = F_z(t)/\sqrt{1-t^2}, \quad F_z(t) = \sum_{N=0}^{\infty} a_N T_N(t), \tag{12a}$$

$$M_x[x(t)] = \sqrt{1-t^2}F_x(t), \quad F_x(t) = \sum_{N=0}^{\infty} b_N U_N(t) \tag{12b}$$

$a_N$, $b_N$ being expansion constants. Using the Galerkin approach one arrives at the infinite linear algebraic system

$$\sum_{N=0}^{\infty}\left(K_{MN}^{xz}a_N+K_{MN}^{xx}b_N\right)=\frac{1}{2}h_x(0+)(c_M-c_{M+2}), \quad (13a)$$

$$\sum_{N=0}^{\infty}\left(K_{MN}^{zz}a_N+K_{MN}^{zx}b_N\right)=h_z(0+)c_M \quad (13b)$$

$(M=0,1,2,\cdots,\infty)$ where

$$K_{MN}^{xx}=\left[I^{11}\left(M,N;G^{(1)}\right)+\sum_{s=0}^{1}\frac{1}{2\omega\mu_s w}D_{MN}^{(1)}\left(k_s^2,\kappa_s w\right)\right]d_{MN}^{+} \quad (14a)$$

$$K_{MN}^{xz}=-K_{NM}^{zx}=\left[I^{10}\left(M,N;G^{(2)}\right)+j\beta\sum_{s=0}^{1}\frac{1}{2\omega\mu_s}C_{MN}^{(1)}(\kappa_s w)\right]d_{MN}^{-} \quad (14b)$$

$$K_{MN}^{zz}=\left[I^{00}\left(M,N;G^{(3)}\right)+w\sum_{s=0}^{1}\frac{\kappa_s^2}{2\omega\mu_s}A_{MN}^{(1)}(\kappa_s w)\right]d_{MN}^{+} \quad (14c)$$

$$d_{MN}^{\pm}=[1\pm(-1)^{M+N}]/2, \quad c_M=\pi J^M J_M(k_x w). \quad (15)$$

Here $J_M(\cdot)$ is the Bessel function, $F_{MN}^{(1)}$ $(F\equiv A,C,D)$ stand for numerically efficient analytical expressions given in [1], and $I^{mn}(M,N,G^{(j)})(m,n=0,1;j=1,2,3)$ are real-axis spectral integrals defined by

$$I^{mn}\left(M,N;G^{(j)}\right)=-\pi w(-1)^M j^{M+N}(M+1)^m(N+1)^n\times\int_0^{\infty}G^{(j)}(u)\frac{J_{M+m}(wu)}{(wu)^m}\frac{J_{N+n}(wu)}{(wu)^n}\,du. \quad (16)$$

The very strong (exponential) convergence of these integrals is a powerful feature which greatly enhances the efficiency of the algorithm.

### B. Disretization of (10) by Method B

The unknowns in this method are the quantities $\{F_z(t_n),F_x(\hat{t}_n);n=1,2,\cdots,L\}$ where $L$ is an integer whereas

$$t_n=\cos[(2n-1)\pi/(2L)], \quad \hat{t}_n=\cos[n\pi/(L+1)]. \quad (17)$$

Proceeding along the lines outlined in [1] one ends up with the linear algebraic system

$$\sum_{n=1}^{L}\left[\tilde{R}_{mn}^{xx}F_x(\hat{t}_n)+\tilde{R}_{mn}^{xz}F_z(t_n)\right]=h_x(0+)\exp(jk_x w\hat{t}_m) \quad (18a)$$

$$\sum_{n=1}^{L}\left[\tilde{R}_{mn}^{zx}F_x(\hat{t}_n)+\tilde{R}_{mn}^{zz}F_z(t_n)\right]=h_z(0+)\exp(jk_x w t_m) \quad (18b)$$

$(m=1,2,\cdots,L)$ where the integer $L$ is sufficiently large to ensure convergence of (21) below. The matrix elements are given by

$$\tilde{R}_{mn}^{xx}=J^a\left(\hat{t}_m,\hat{t}_n;G^{(1)}\right)+\frac{1}{j\omega\pi w}\sum_{s=0}^{1}\frac{1}{\mu_s}\tilde{D}_{mn}^{(1)}\left(k_s^2,\kappa_s w\right) \quad (19a)$$

$$\tilde{R}_{mn}^{xz}=J^b\left(\hat{t}_m,t_n;G^{(2)}\right)+\frac{\beta}{\omega\pi}\sum_{s=0}^{1}\frac{1}{\mu_s}\tilde{C}_{mn}^{(1)}(\kappa_s w) \quad (19b)$$

$$\tilde{R}_{mn}^{zx}=J^a\left(t_m,\hat{t}_n;G^{(2)}\right)+\frac{\beta}{\omega\pi}\sum_{s=0}^{1}\frac{1}{\mu_s}\tilde{B}_{mn}^{(1)}(\kappa_s w) \quad (19c)$$

$$\tilde{R}_{mn}^{zz}=J^b\left(t_m,t_n;G^{(3)}\right)+\frac{w}{j\omega\pi}\sum_{s=0}^{1}\frac{\kappa_s^2}{\mu_s}\tilde{A}_{mn}^{(1)}(\kappa_s w). \quad (19d)$$

Here, $J^a$ and $J^b$ are exponentially converging spectral integrals defined by

$$J^a(t,\hat{t}_n;G)=\frac{w}{2(L+1)}(1-\hat{t}_n^2)J^c(t,\hat{t}_n;G),\qquad J^b(t,t_n;G)=\frac{w}{2L}J^c(t,t_n;G); \quad (20a)$$

$$J^c(t,\tau;G)=\int_{-\infty}^{\infty}G(u)\exp[-jw(t-\tau)u]\,du. \quad (20b)$$

On the other hand, $\tilde{F}_{mn}^{(1)}$ $(F\equiv A,B,C,D)$ are most efficiently given either in closed form or in terms of simple single series in [1].

In terms of $\{F_z(t_n),F_x(\hat{t}_n)\}$ the distribution of surface magnetic currents may be found from (12) with the help of [1]

$$F_x(t)=\frac{2}{L+1}\sum_{N=0}^{L-1}\sum_{n=1}^{L}(1-\hat{t}_n^2)U_n(\hat{t}_n)U_N(t)F_x(\hat{t}_n) \quad (21a)$$

$$F_z(t)=\frac{1}{L}\sum_{N=0}^{L-1}(2-\delta_{N0})\sum_{n=1}^{L}T_N(t_n)T_N(t)F_z(t_n) \quad (21b)$$

$(\delta_{N0}=0$ if $N\neq 0,\delta_{00}=1)$.

*Note:* In the case $m=n=0$ (a slot separating two dielectric half spaces), $G^{(1)}=G^{(2)}=G^{(3)}=0$ and, thus, all spectral integrals in (14) and (19) vanish. In this case, therefore, all matrix elements assume completely analytical expressions in the context of both methods A and B.

## IV. Reduction of (6) to a System of SIE-SIDE

For the same reasons explained in connection with (3), system (6), connected with the structure of Fig. 1(b), is also rather impractical. To recast it into a convenient form one may use the decompositions

$$\frac{1}{\Psi^q(u)}=\frac{1}{\mathcal{Y}_1^q+\mathcal{Y}_0^q}+P^q(u) \quad (q\equiv e,h)$$
$$Z_j(u)=\mathcal{Z}_j(u)+Z^{(j)}(u) \quad (22)$$

where

$$\mathcal{Z}_j(u)=Z_j\left(u;\mathcal{Y}_1^e+\mathcal{Y}_0^e,\mathcal{Y}_1^h+\mathcal{Y}_0^h\right)$$
$$Z^{(j)}(u)=Z_j\left(u;\frac{1}{P^e},\frac{1}{P^h}\right) \quad (23)$$

$(j = 1,2,3)$. One observes that $P^q(u)$ as well as $Z^j(u)$ decay very strongly (exponentially) as $u \to \pm\infty$, whereas $\mathcal{Z}_j(u)$ continue to vary as $|u|^{2-j}$, i.e., rather inconveniently. By properly handling the inverse Fourier integrals $\int_{-\infty}^{\infty} \mathcal{Z}_j(u)\, e^{-ju(x-x')}\, du$ as outlined in [1] one arrives at the system

$$\mathcal{K}^J(R_1,R_2;x) + \left(k_A^2 \frac{d^2}{dx^2} + k_C^2\right)\mathcal{J}_x^1(x) + \left(k_B^2 \frac{d^2}{dx^2} + k_D^2\right)\mathcal{J}_x^2(x) + j\beta \frac{d}{dx}\left[k_A^2 \mathcal{J}_z^1(x) + k_B^2 \mathcal{J}_z^2(x)\right] = e_x(0+)\, e^{jk_x x} \tag{24a}$$

$$\mathcal{K}^J(R_2,R_3;x) + j\beta \frac{d}{dx}\left[k_A^2 \mathcal{J}_x^1(x) + k_B^2 \mathcal{J}_x^2(x)\right] - T_A \mathcal{J}_z^1(x) - T_B \mathcal{J}_z^2(x) = e_z(0+)\, e^{jk_x x} \tag{24b}$$

$(|x| \le w)$. Here

$$\mathcal{J}_p^1(x) = \int_{-w}^{w} J_p(x') H_0^{(2)}(\kappa_1 |x-x'|)\, dx'$$
$$\mathcal{J}_p^2(x) = \int_{-w}^{w} J_p(x') K(|x-x'|)\, dx' \quad (p \equiv x,z) \tag{25}$$

$$K(|x-x'|) = -\frac{1}{\kappa_1^2 - \kappa_0^2} \sum_{s=0}^{1} (-1)^s \kappa_s^2 \left[H_0^{(2)}(\kappa_s |x-x'|) + H_2^{(2)}(\kappa_s |x-x'|)\right]. \tag{26}$$

The quantities $R_j (j = 1,2,3)$ (rapidly converging functions of the spectral variable $u$), $k_P^2 (P \equiv A,B,C,D)$, and $T_Q (Q \equiv A,B)$ are defined in Appendix B.

### A. Discretization of (24) Using Method A

Setting $x = wt$, $x' = wt'$, $J_z[x(t)] = F_z(t)/\sqrt{1-t^2}$, $J_x[x(t)] = \sqrt{1-t^2} F_x(t)$, and expanding $F_z$ and $F_x$ according to (12), we again obtain the system (13) with $e_p(0)$ in place of $h_p(0+)$; $p \equiv x,z$. Now

$$K_{MN}^{xx} = \left\{ -I^{11}(M,N;R_1) + \frac{1}{w}\left[k_A^2 D_{MN}^{(1)}\left(k_C^2/k_A^2, \kappa_1 w\right) + k_B^2 D_{MN}^{(2)}\left(k_D^2/k_B^2, \kappa_1 w, \kappa_0 w\right)\right]\right\} d_{MN}^{+} \tag{27a}$$

$$K_{MN}^{xz} = -K_{NM}^{zx} = \left\{ -I^{10}(M,N;R_2) + j\beta\left[k_A^2 C_{MN}^{(1)}(\kappa_1 w) + k_B^2 C_{MN}^{(2)}(\kappa_1 w, \kappa_0 w)\right]\right\} d_{MN}^{-} \tag{27b}$$

$$K_{MN}^{zz} = \left\{ -I^{00}(M,N;R_3) - w\left[T_A A_{MN}^{(1)}(\kappa_1 w) + T_B A_{MN}^{(2)}(\kappa_1 w, \kappa_0 w)\right]\right\} d_{MN}^{+}. \tag{27c}$$

The quantities $F_{MN}^{(2)}$ $(F \equiv A,C,D)$ are given in [1] in an efficient analytical form. On the other hand, $I^{mn}(M,N;R_j) = j\omega\varepsilon_1 I^{mn}(M,N;Z^{(j)}) + I^{mn}(M,N;R^{(j)})$ where the first term is exponentially converging while the second converges as $1/u^6$.

### B. Discretization of (24) Using Method B

Using method B we obtain again the linear algebraic system (18) with $e_p(0)$ in place of $h_p(0+)$: $p \equiv x,z$. Now

$$\tilde{R}_{mn}^{xx} = J^a(\hat{t}_m, \hat{t}_n; R_1) + \frac{2}{j\pi w}\left[k_A^2 \tilde{D}_{mn}^{(1)}\left(k_C^2/k_A^2, \kappa_1 w\right) + k_B^2 \tilde{D}_{mn}^{(2)}\left(k_D^2/k_B^2, \kappa_1 w, \kappa_0 w\right)\right] \tag{28a}$$

$$\tilde{R}_{mn}^{xz} = J^b(\hat{t}_m, t_n; R_2) + \frac{2}{\pi}\beta\left[k_A^2 \tilde{C}_{mn}^{(1)}(\kappa_1 w) + k_B^2 \tilde{C}_{mn}^{(2)}(\kappa_1 w, \kappa_0 w)\right] \tag{28b}$$

$$\tilde{R}_{mn}^{zx} = J^a(t_m, \hat{t}_n; R_2) + \frac{2}{\pi}\beta\left[k_A^2 \tilde{B}_{mn}^{(1)}(\kappa_1 w) + k_B^2 \tilde{B}_{mn}^{(2)}(\kappa_1 w, \kappa_0 w)\right] \tag{28c}$$

$$\tilde{R}_{mn}^{zz} = J^b(t_m, t_n; R_3) - \frac{2w}{j\pi}\left[T_A \tilde{A}_{mn}^{(1)}(\kappa_1 w) + T_B \tilde{A}_{mn}^{(2)}(\kappa_1 w, \kappa_0 w)\right]. \tag{28d}$$

$\tilde{F}_{mn}^{(2)}$ $(F \equiv A,B,C,D)$ are given in [1] either in closed form or in terms of simple single series, solely. On the other hand, $J^q(t,\tau;R_j) = j\omega\varepsilon_1 J^q(t,\tau;Z^{(j)}) + J^q(t,\tau;R^{(j)})$ $(q \equiv a,b; j = 1,2,3)$ where $J^q(t,\tau;Z^{(j)})$ are exponentially converging while $J^q(t,\tau;R^{(j)})$ converge uniformly as $1/|u|^{3+j}$.

In terms of $\{F_x(\hat{t}_n), F_z(t_n)\}$ $F_x(t)$ and $F_z(t)$ are evaluated again from (21).

## V. Far-Scattered Field

*Notation:* The symbol $i$ is used throughout this section to designate any of the outmost regions $(-n-1)$ or $(m+1)$.

In the system of cylindrical coordinates $O(\rho,\phi,z)$ where $\phi$ is measured from the $y$ axis counterclockwise, the far-scattered field radiated at $\bar{r}(\rho,\phi,z) \in (i)$ is given by

$$\bar{E}(\rho,\phi,z) = \sqrt{j2\pi\kappa_i/\rho}\cos\phi\, e^{-jk_i\rho + j\beta z} \times \left[\hat{z}\mathcal{E}_z^i + \hat{\rho}\frac{\beta}{\kappa_i}\mathcal{E}_z^i + \hat{\phi}\left(\mathcal{E}_x^i - \frac{\beta}{\kappa_i}\sin\phi\,\mathcal{E}_z^i\right)\frac{1}{\cos\phi}\right] \tag{29}$$

$$\bar{H}(\rho,\phi,z) = \frac{1}{\omega\mu_i}\bar{k}_i \times \bar{E}(\rho,\phi,z), \quad \bar{k}_i = -\beta\hat{z} + \kappa_i\hat{\rho}. \tag{30}$$

Here $\mathcal{E}_p^i = \tilde{E}_p(u,y)$ $(p \equiv x,z)$, the Fourier transforms with respect to $x$ of $E_p(x,y)$ are evaluated as in Appendix A at $u = u_i = \kappa_i \sin\phi$, $y = y_i$ $(= h_m$ when $i = m+1$, $h_{-n-1}$ when $i = -n-1)$.

The power $P_{\text{rad}}$ carried by the space-wave part of the far-scattered field is given by

$$P_{\text{rad}} = P_{\text{rad}}^{(m+1)} + P_{\text{rad}}^{(-n-1)}. \tag{31a}$$

Here

$$P_{\text{rad}}^{(i)} = \int_{C_i} U^i(\phi)\, d\phi, \quad U^i(\phi) = \frac{\pi\kappa_i^2}{\omega\mu_i}\cos^2\phi\left[\left|\mathcal{E}_x^i\right|^2 + \left|\mathcal{E}_z^i\right|^2 + \left|\frac{u_i\mathcal{E}_x^i - \beta\mathcal{E}_z^i}{\kappa_i\cos\phi}\right|^2\right] \tag{31b}$$

if $\kappa_i^2 > 0$, otherwise $P_{\text{rad}}^{(i)} = 0$ $(i = -n-1$ or $i = m+1)$. $C_i$ in (31) denotes the intervals $-\frac{\pi}{2} < \phi < \frac{\pi}{2}$ (if $i = m+1$), $\frac{\pi}{2} < \phi < 3\frac{\pi}{2}$ (if $i = -n-1$).

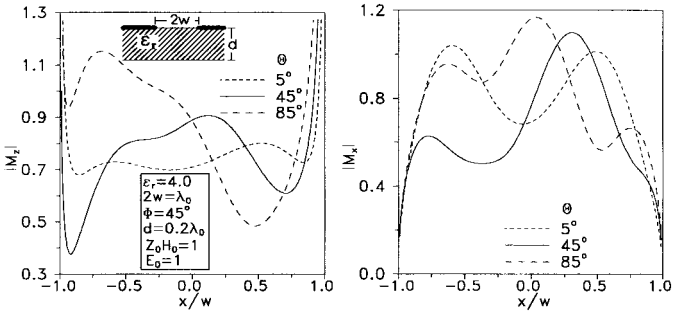


Fig. 2. Equivalent surface magnetic current densities across a slot on the top surface of a dielectric slab. (a) $|M_z|$. (b) $|M_x|$.

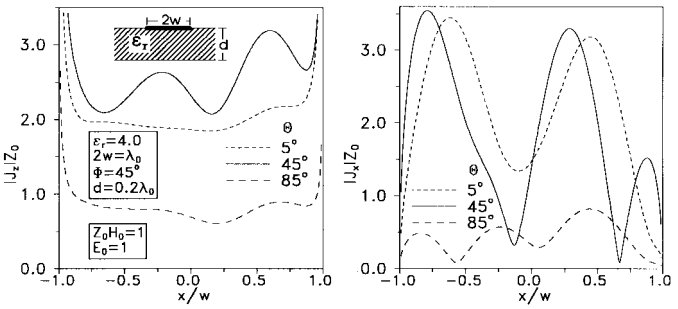


Fig. 3. Normalized current densities induced on a strip right on the top surface of a dielectric slab. (a) $|J_z|Z_o$. (b) $|J_x|Z_o$.

The total scattered power (radiation plus surface wave, if any) may be found by integrating the Poynting vector over the cross section of the strip/slot. The final result is

$$P_{\text{scat}} = \frac{w}{2}\,\text{Re}\sum_{M=0}^{\infty}\left(b_M^* c_M^x + a_M^* c_M^z\right) \tag{32}$$

where $c_M^x$ and $c_M^z$ denote, respectively, the right side of (13a) and (13b) [taking into account the modifications mentioned just before (27a), in the case of the structure of Fig. 1(b)]. For $m = 0 = n$ (single-layered structures) (31) and (32) must yield coinciding results. This equality of results, which has been used as a partial check of the validity of the numerical codes, has been ascertained to within 13 significant decimals in all cases that have been considered.

## VI. Numerical Results and Discussion

Fig. 2 shows typical results for the equivalent surface magnetic current density across an open microslot-line for $2w = \lambda_0$ ($\lambda_0$ is the free-space wavelength), $E_0 = 1 = Z_0H_0$ ($Z_0$ is the free-space wave impedance), $\Phi = 45°$, and for three values of $\Theta$ $(5°, 45°, 85°)$. Fig. 3 shows the normalized current densities $|J_z|Z_0$ and $|J_x|Z_0$ induced on a strip right on the top surface of a dielectric slab, while in Fig. 4 the slab is grounded. The frequency is taken to be 10 GHz in all cases whereas the magnetic permeability of all regions is taken to be that of free-space. As a partial test of their correctness, results in all Figs. 2–4 have been independently derived by methods

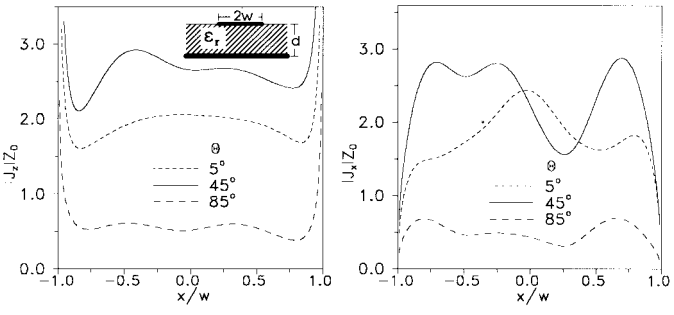


Fig. 4. Normalized current densities induced on a strip right on the surface of a grounded dielectric slab. (a) $|J_z|Z_o$. (b) $|J_x|Z_o$.

TABLE I
Radiated Power of (31) and Scattered Power of (32) for a Slot Between Air and a Dielectric Half-Space with Relative Dielectric Constant $\varepsilon_r = 2$ $(2w = \lambda_0/2, \Phi = \Theta = 45°, E_0 = Z_0H_0 = 1)$

| $N_r$ | $P_{rad}$ of (31) | $P_{scat}$ of (32) |
|---|---|---|
| 5 | $7.0275433047637097\times10^{-5}$ | $7.0275433047637084\times10^{-5}$ |
| 10 | $7.0275434383853202\times10^{-5}$ | $7.0275434383853188\times10^{-5}$ |
| 15 | $7.0275434383853202\times10^{-5}$ | $7.0275434383853188\times10^{-5}$ |

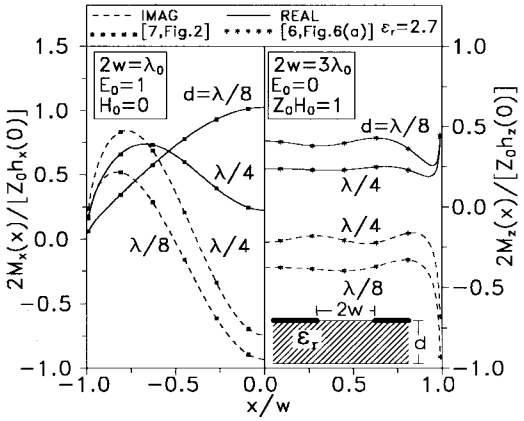


Fig. 5. Normalized equivalent surface magnetic currents on a slot right on the top surface of a dielectric slab for several slab widths ($d = \lambda/8, \lambda/4$; $\lambda$ is the wavelength in the dielectric). The excitations are normally incident TE or TM (to slot axis) plane waves.

A and B. As a further test, the results in Table I ascertain the energy conservation principle to within 13 decimals in the case of a single slot separating two half-spaces [see comments after (32)]. The entry $N_r$ in this table stands for the number of terms used in each of (12).

In addition to the above internal checks, extensive comparisons with previously published results have been also carried out in the special case of normal incidence ($\Phi = 90°$). Some typical results of this comparison are shown in Fig. 5 for an open microslot line and reveal an excellent agreement with corresponding ones taken from [6]–[7]. (We also reproduced all curves of [6, Figs. 5, 6], [7, Figs. 2, 3], [10, Figs. 2–7] (not shown), noticing that $2w/\lambda_b$ in [10] should read as $2w/\lambda_a$). In the case of a strip right on the surface of a dielectric slab (either grounded or surrounded by air), the computer programs developed here have also been tested with the help of the numerical codes of [8] and [9].

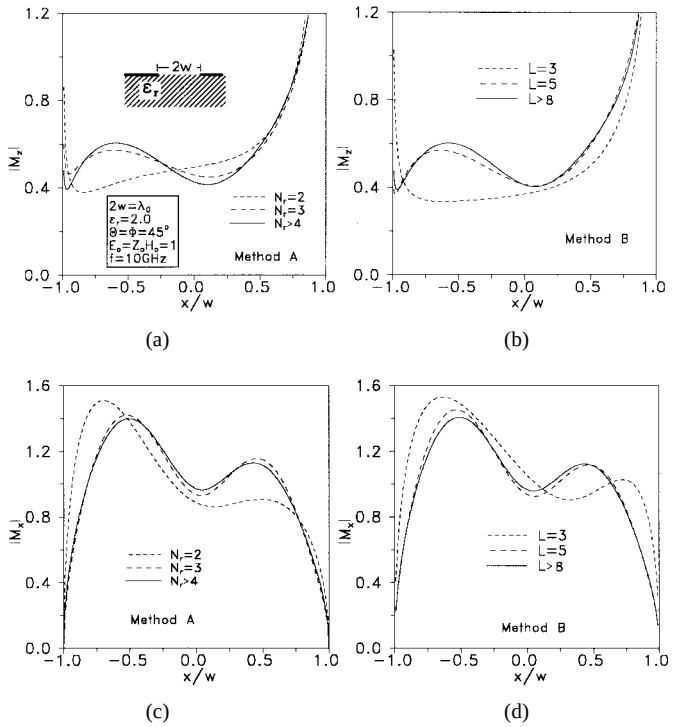


Fig. 6. Convergence of the algorithms for the equivalent surface magnetic current densities across a slot separating two dielectric half-spaces. (a) and (c) Method A. (b) and (d) Method B.

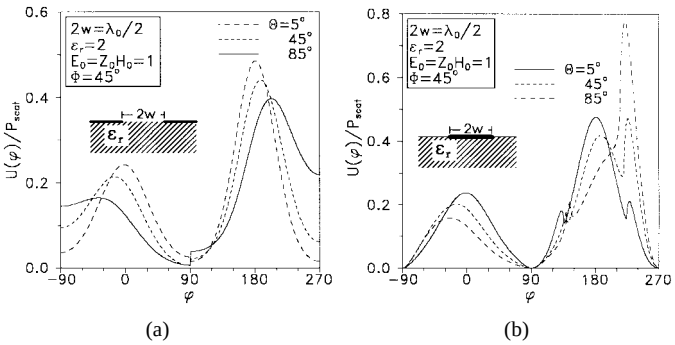


Fig. 7. Normalized radiation intensities for (a) a slot and (b) a strip right on the interface between two dielectric half-spaces for several angles of incidence.

To appreciate the convergence characteristics of both methods A and B, Fig. 6 shows $|M_z|$ and $|M_x|$ versus $x$ for several values of $N_r$ (the number of basis functions used in each of (12), method A) or $L$ (method B). As seen both methods yield indistinguishable final results. Method A, however, converges more rapidly.

Finally, in Fig. 7 we show the normalized radiation intensity $U(\phi)/P_{\text{scat}}$ versus $\phi$ for a slot [Fig. 7(a)] or a strip [Fig. 7(b)] right on the interface between two half-spaces for several angles of incidence. $U(\phi)$ has been defined in (31b) for $-\frac{\pi}{2} < \phi < 3\frac{\pi}{2}$.

*Note:* By the algorithms developed here, one can treat in a unified fashion any layered strip- or slot-loaded, structure. In this respect, perfectly conducting regions (for example ground planes in microstrip or microslot lines) can be accounted for simply by equating to zero their impedances $\zeta^e$ and $\zeta^h$, defined in (39).

## VII. Conclusion

Two independent, direct singular integral equation techniques outlined in [1] were used here to analyze advantageously three-dimensional scattering by strip/slot-loaded planar structures. This novel approach enables one to arrive at linear algebraic systems whose matrix elements are given by rapidly convergent real-axis spectral integrals. The numerical codes have been exhaustively tested by several internal and external checks.

## Appendix A

*Description of the Immittance-Like Formulation Technique:* In the Fourier transform domain

$$\tilde{f}(u,y) = \frac{1}{2\pi}\int_{-\infty}^{\infty} f(x,y)\, e^{jux}\, dx$$
$$f(x,y) = \int_{-\infty}^{\infty} \tilde{f}(u,y)\, e^{-jux}\, du \tag{33}$$

let us define

$$\tilde{E}_e^{(i)}(u,y) = u\tilde{E}_x(u,y) - \beta\tilde{E}_z(u,y)$$
$$\tilde{E}_h^{(i)}(u,y) = \beta\tilde{E}_x(u,y) + u\tilde{E}_z(u,y) \tag{34a}$$

$$\tilde{H}_h^{(i)}(u,y) = u\tilde{H}_x(u,y) - \beta\tilde{H}_z(u,y)$$
$$\tilde{H}_e^{(i)}(u,y) = \beta\tilde{H}_x(u,y) + u\tilde{H}_z(u,y) \tag{34b}$$

where the superscript $(i)$ is used to designate the $i$th region in each of the structures of Fig. 1 ($-n-1 \le i \le m+1$). Then $\tilde{E}_q^{(i)}$ and $\tilde{H}_q^{(i)}$ $(q \equiv e,h)$ satisfy dual decoupled equations

$$\tilde{E}_e^{(i)}(u,y) = -j(u^2+\beta^2)\frac{d}{dy}\tilde{\Pi}_e^{(i)}(u,y)$$
$$\tilde{E}_h^{(i)}(u,y) = -\omega\mu_i(u^2+\beta^2)\tilde{\Pi}_h^{(i)}(u,y) \tag{35a}$$

$$\tilde{H}_h^{(i)}(u,y) = -j(u^2+\beta^2)\frac{d}{dy}\tilde{\Pi}_h^{(i)}(u,y),$$
$$\tilde{H}_e^{(i)}(u,y) = \omega\varepsilon_i(u^2+\beta^2)\tilde{\Pi}_e^{(i)}(u,y) \tag{35b}$$

when the representation in terms of the Hertzian potentials $\hat{y}\Pi_e(x,y)\, e^{j\beta z}$ and $\hat{y}\Pi_h(x,y)\, e^{j\beta z}$ is used for the scattered field. These potentials, satisfying homogeneous Helmholtz's equations, are given by

$$\tilde{\Pi}_q^{(m+1)}(u,y) = A_q^{(m+1)}(u)\, e^{-\gamma_{m+1}(y-h_m)} \tag{36a}$$
$$\tilde{\Pi}_q^{(-n-1)}(u,y) = A_q^{(-n-1)}(u)\, e^{\gamma_{-n-1}(y-h_{-n-1})} \tag{36b}$$
$$\tilde{\Pi}_q^{(i)}(u,y) = A_q^{(i)}(u)\cosh[\gamma_i(y-h_i)] + B_q^{(i)}(u) \times \sinh[\gamma_i(y-h_i)] \quad (-n \le i \le m) \tag{36c}$$

$q \equiv e,h$. Here, $A_q^{(i)}$ and $B_q^{(i)}$ denote expansion constants

$$\gamma_i = \gamma_i(u) = \sqrt{u^2-\kappa_i^2}, \quad \kappa_i^2 = k_i^2 - \beta^2 \tag{37}$$

$-\frac{\pi}{2} < \arg(\gamma_p) \le \frac{\pi}{2}$ ($p = -n-1$ or $p = m+1$) (radiation condition). Let

$$Z^q(u,y) = 1/Y^q(u,y) = \tilde{E}_q^{(i)}(u,y)/\tilde{H}_q^{(i)}(u,y) \quad (q \equiv e,h) \tag{38}$$

$$\zeta_i^e = 1/\mathcal{Y}_i^e = j\gamma_i/(\omega\varepsilon_i), \zeta_i^h = 1/\mathcal{Y}_i^h = j\omega\mu_i/\gamma_i \tag{39}$$

where, for $y \neq 0$, $Z^q(u,y)$ and $Y^q(u,y)$ are continuous functions of $y$. Then

$$F^q(u,h_m+0) = f^q_{m+1}, F^q(u,h_{-n-1}-0) = -f^q_{-n-1} \quad (40a)$$

$$F^q(u,h_{i-1}+) = f^q_i \frac{F^q(u,h_i-) + f^q_i \tanh(\gamma_i D_i)}{f^q_i + F^q(u,h_i-)\tanh(\gamma_i D_i)} \quad (-n \le i \le m) \quad (40b)$$

$$F^q(u,h_i-) = f^q_i \frac{F^q(u,h_{i-1}+) - f^q_i \tanh(\gamma_i D_i)}{f^q_i - F^q(u,h_{i-1}+)\tanh(\gamma_i D_i)} \quad (-n \le i \le m) \quad (40c)$$

$F \equiv Z,\ Y; f \equiv \zeta, \mathcal{Y}$. Equation (40) enable one to obtain $Y^q(u,h_i)$ recursively for any $i$.

*Derivation of (3) and (6):* In connection with both structures in Fig. 1, using (38) one readily gets

$$\tilde{H}^{(i)}_q(u,0+) - \tilde{H}^{(0)}_q(u,0-) = \Psi^q(u)\tilde{E}_q(u) \quad (q \equiv e,h) \quad (41)$$

where $\tilde{E}_q(u) = \tilde{E}^{(1)}_q(u,0+) = \tilde{E}^{(0)}_q(u,0-)$

$$\Psi^q(u) = Y^q(u,0+) - Y^q(u,0-) \quad (q \equiv e,h) \quad (42)$$

with $Y^q(u,0+)\backslash Y^q(u,0-)$ evaluated from (40b)\(40c) downwards\upwards. We use (34) to express $\tilde{E}_q(u)$, $\tilde{H}^{(0)}_q(u,0-)$, and $\tilde{H}^{(1)}_q(u,0+)$ $(q \equiv e,h)$ in terms of $\tilde{E}_t$ and $\tilde{H}_t$ $(t \equiv x,z)$ and then substitute into (41). Taking the inverse Fourier transform of both sides of the resulting equations and applying the continuity of the $x$ and $z$ components of the total (i.e., scattering plus excitation) magnetic field across the slot the system of integral equations (3) is obtained. System (6) may be obtained in a similar manner.

*Evaluation of $\tilde{E}_p(u,h_m)$ and $\tilde{E}_p(u,h_{-n-1})$ $(p \equiv x,z)$ in (29):* We refer to the structure of Fig. 1(a). Beginning with the relations

$$\tilde{E}_x(u,0) \equiv \tilde{M}_z(u) = \frac{w}{2}\sum_{n=0}^{\infty} a_n j^n J_n(wu)$$

$$-\tilde{E}_z(u,0) \equiv \tilde{M}_x(u) = \frac{w}{2}\sum_{n=0}^{\infty} b_n j^n (n+1)\frac{J_{n+1}(wu)}{uw}$$

[where $a_n$, $b_n$ are known from the solution of (13)] we successively evaluate $\tilde{E}^{(0)}_q(u,0) = \tilde{E}^{(1)}_q(u,0)$ $(q \equiv e,h)$ from (34a), $\tilde{H}^{(1)}_e(u,0+)$ and $\tilde{H}^{(0)}_e(u,0-)$ from (38), $\tilde{\Pi}^{(0)}_q(u,0-)$ and $\tilde{\Pi}^{(1)}_q(u,0+)$ from the second of each of (35a) and (35b). We next use the relation implied by (36c)

$$\tilde{\Pi}^{(i)}_q(u,y) = \tilde{\Pi}^{(i)}_q(u,h_i)\{\cosh[\gamma_i(y-h_i)] - \lambda_q \sinh[\gamma_i(y-h_i)]\} \quad (-n \le i \le m)$$

(where $\lambda_e = Z^e(u,h_i)/\zeta^e_i, \lambda_h = Y^h(u,h_i)/\mathcal{Y}^h_i$) as well as

$$\varepsilon_i \tilde{\Pi}^{(i)}_e(u,h_i) = \varepsilon_{i+1}\tilde{\Pi}^{(i+1)}_e(u,h_i)$$
$$\mu_i \tilde{\Pi}^{(i)}_h(u,h_i) = \mu_{i+1}\tilde{\Pi}^{(i+1)}_h(u,h_i)$$

starting from $\{i=1,\ y=0+\}\backslash\{i=0,\ y=0-\}$ to evaluate $\tilde{\Pi}^{(m+1)}_q(u,h_m)\backslash\tilde{\Pi}^{(-n-1)}_q(u,h_{-n-1})$ $(q \equiv e,h)$. Then we use again the second of each of (35a) and (35b) to find $\tilde{E}^{(m+1)}_q(u,h_m)$, $\tilde{E}^{(-n-1)}_q(u,h_{-n-1})$ $(q \equiv e,h)$ and, finally, in terms of them, the sought values using (34a). The case of the structure in Fig. 1(b) is treated in a similar manner.

## APPENDIX B

*Expressions of $R_j$ $(j=1,2,3)$, $k^2_P$ $(P \equiv A,B,C,D)$, $T_Q$ $(Q \equiv A,B)$:* Let

$$\varepsilon = \frac{\varepsilon_0}{\varepsilon_1}, \quad \mu = \frac{\mu_0}{\mu_1}, \quad \xi_1 = \frac{1-\mu^2}{\varepsilon-\mu}$$
$$\xi_2 = \frac{\varepsilon\mu - 1}{\varepsilon - \mu}, \quad \xi_3 = \frac{\mu^2\kappa_1^2 - \kappa_0^2}{\varepsilon - \mu} \quad (43)$$

$$A_p = \frac{2(p-1)}{(p+1)^2}, \quad B_p = \frac{4}{(p+1)^2}$$
$$F_p(u) = \frac{\left(k_1^2 - k_0^2\right)^2}{\gamma_1(\gamma_1+\gamma_0)^3(\gamma_0 + p\gamma_1)} \quad (p \equiv \varepsilon,\mu). \quad (44)$$

Then

$$k^2_A = \xi_1 A_\mu + \xi_2 A_\varepsilon, \quad k^2_B = \xi_1 B_\mu + \xi_2 B_\varepsilon, \quad k^2_C = \mu k_1^2 A_\mu,$$
$$k^2_D = \mu k_1^2 B_\mu; \quad T_Q = \xi_3 Q_\mu + \beta^2 \xi_2 Q_\varepsilon \quad (Q \equiv A,B) \quad (45)$$

$$R_1 = 4\omega\varepsilon_1 Z^{(1)} + R^{(1)}, \quad R^{(1)} = 2j\{[\xi_1 A_\mu F_\mu(u) + \xi_2 A_\varepsilon F_\varepsilon(u)]u^2 - k_1^2 \mu A_\mu F_\mu(u)\} \quad (46)$$

$$R_2 = 4\omega\varepsilon_1 Z^{(2)} + R^{(2)}, \quad R^{(2)} = -2j\beta u[\xi_1 A_\mu F_\mu(u) + \xi_2 A_\varepsilon F_\varepsilon(u)] \quad (47)$$

$$R_3 = 4\omega\varepsilon_1 Z^{(3)} + R^{(3)}, \quad R^{(3)} = 2j[\xi_3 A_\mu F_\mu(u) + \beta^2 \xi_2 A_\varepsilon F_\varepsilon(u)] \quad (48)$$

with $Z^{(j)}$ $(j=1,2,3)$ defined in the second of (23).

## REFERENCES


[1] J. L. Tsalamengas, "Direct singular integral equation methods in scattering and propagation in strip or slot loaded structures," *IEEE Trans. Antennas Propagat*, vol. 46, pp. 1560–1570, Oct. 1998.

[2] T. Itoh, *Numerical Techniques for Microwave and Millimeter-Wave Passive Structures*. New York: Wiley, 1989.

[3] R. W. P. King and T. T. Wu, *The Scattering and Diffraction of Waves*. Cambridge, MA: Harvard Univ. Press, 1959.

[4] D. S. Jones, *The Theory of Electromagnetism*. Oxford, U.K.: Pergamon, 1964.

[5] K. A. Michalski and C. M. Butler, "Determination of current induced on a conducting strip embedded in a dielectric slab," *Radio Sci.*, vol. 18, no. 6, pp. 1195–1206, Nov./Dec. 1983.

[6] R. E. Nevels and C. M. Butler, "Electromagnetic diffraction by a slot in a ground screen covered by a dielectric slab," *IEEE Trans. Antennas Propagat.*, vol. AP-30, pp. 390–395, May 1982.

[7] ——, "Electromagnetic penetration through a slot in a screen covered by a dielectric slab," *Electromagn.*, vol. 2, pp. 147–159, 1982.

[8] J. L. Tsalamengas and J. G. Fikioris, "TM-scattering by conducting strips right on the planar interface of a three-layered medium," *IEEE Trans. Antennas Propagat.*, vol. 45, pp. 542–555, May 1993.

[9] J. L. Tsalamengas, "TE-scattering by conducting strips right on the planar interface of a three-layered medium," *IEEE Trans. Antennas Propagat.*, vol. 45, pp. 1650–1658, Dec. 1993.

[10] C. M. Butler, "Current induced by a conducting strip which resides on the planar interface between two semi-infinite half-spaces," *IEEE Trans. Antennas Propagat.*, vol. AP-32, pp. 226–231, Mar. 1984.

[11] C. A. Balanis, *Advanced Engineering Electromagnetics*. New York: Wiley, 1989.


**John. L. Tsalamengas** (M'87), for photograph and biography, see p. 555 of the May 1993 issue of this TRANSACTIONS.